Journal of Molecular Graphics and Modelling 29 (2011) 763–772

Contents lists available at ScienceDirect

Journal of Molecular Graphics and Modelling

journal homepage: www.elsevier.com/locate/JMGM

Development of quantitative structure–activity relationships for explanatory modeling of fast reacting (meth)acrylate monomers bearing novel functionality

Jason A. Morrill[a,*], Joedd H. Biggs[a], Christopher N. Bowman[b], Jeffrey W. Stansbury[c]

[a] Department of Chemistry, William Jewell College, 500 College Hill, Liberty, MO 64068, United States
[b] Department of Chemical and Biological Engineering, University of Colorado, Boulder, CO 80309, United States
[c] School of Dentistry, University of Colorado Health Sciences Center, Biomaterials Research Center, 12800 E 19th Street, Aurora, CO 80010, United States

ARTICLE INFO

Article history:
Received 29 September 2010
Accepted 23 December 2010
Available online 8 January 2011

Keywords:
QSAR
Polymerization
Reactivity
Acrylate
AM1

ABSTRACT

The photoinitiated polymerization of (meth)acrylate monomers bearing novel carbamate functionality exhibits significantly greater reaction rate when compared to more traditional acrylate monomers undergoing similar polymerization. This unusually fast reactivity has been the subject of much investigation. In order to suggest an explanatory mechanism for the enhanced polymerization rates we have conducted quantitative structure–activity relationship investigations of these novel monomers. These studies have resulted in statistically sound models with coefficients of multiple determination of $R^2 > 0.93$. Principal component and k nearest neighbor similarity analysis were also conducted on the multiple regression models. These results are discussed in light of published experimental investigations of the photopolymerization reactivity of the novel monomers.

1. Introduction

The reactivity of a monomer toward photoinitiated radical polymerization exhibits variable dependence on a number of factors not limited to polymerization reaction conditions, the exact formulation of the reaction mixture, and monomer functionality [1]. A complicating factor in the investigation of photopolymerization reactivity is the variety of different reactions taking place throughout the polymerization process. Despite the difficulties in investigating the specific polymerization mechanism, the photopolymerization of acrylate monomers has attracted a great deal of attention due to its utility in a wide variety of applications including adhesives, photolithography, polymeric membranes, biomaterials, and dental materials. The successful development of polymeric materials for any application requires an understanding of both structure–property relationships and structure–reactivity relationships. Should the polymerization reaction be too slow or not proceed to completion, the resulting polymer will very likely lack the designed critical performance properties.

Acrylate monomers have attracted attention in many applications due to acceptable polymeric properties and their tendency to undergo photoinitiated polymerization. In particular, acrylate type monomers having so called novel functionality are interesting because they exhibit unusually fast photopolymerization reactivity. The pioneering work in this area was done by Decker in the RT-NIR investigation [2] of monomers bearing novel functionalities including oxazolidones [3], carbonates [4], cyclic carbonates [5], and carbamates [6]. The reasons for the enhanced reactivity of these types of monomers are not fully understood and the subject of elevated novel acrylate reactivity, in general, has been the subject of much investigation. In multifunctional acrylate monomers it was found that the inclusion of sulfur heteroatoms enhanced photopolymerization reactivity [1]. Bowman found that the presence of a liquid crystalline phase could enhance the photopolymerization reactivity of monoacrylates by segregating reactive monomers into a smaller volume and thereby inducing an ordering effect [7]. For monoacrylates Jansen found evidence that, for capable monomers, hydrogen bonding enhanced polymerization rate, also suggesting an ordering effect [8]. For monomers not capable of hydrogen bonding a positive correlation between the maximum polymerization rate ($R_{p\,max}$) and a Boltzmann-averaged dipole moment that was computed using the AM1 semiempirical quantum mechanical method. The Boltzmann averaging involved a conformational analysis on the rotatable bonds in each of the monomers of the study. Using the enthalpies of formation as weights, the computed dipole moment of each retained conformation was weighted as a probability function with respect to the global minimum energy conformation for each monomer. The result was a com-

* Corresponding author. Tel.: +1 816 415 7874; fax: +1 816 415 5024.
E-mail address: morrillj@william.jewell.edu (J.A. Morrill).

1093-3263/$ – see front matter © 2011 Published by Elsevier Inc.
doi:10.1016/j.jmgm.2010.12.009

posite computed dipole moment that was found to be positively correlated with $R_{p\,max}$ for both neat monomers and monomers in solutions at varying concentrations, although the method of computing the dipole moment of a mixture of monomers was not described. In an effort to further elucidate the relationships between monomer structure and reactivity Bowman et al. examined a series of (meth)acrylate monomers dominated by carbamate and carbonate secondary functionality as so-called "end-groups" connected to the acrylate by an ethyl spacer [9]. The monomers were designed to explore the hypothesized roles of hydrogen bonding, hydrogen abstraction, and electronic effects. The authors noted that each of these effects is important in affecting the monomer reactivity to varying extents depending on the monomer functionality and substitution. Specifically, the role hydrogen bonding was investigated using melting point considerations and variable temperature FTIR analysis of the N–H stretching bands. The authors found no evidence that directly supported the role of hydrogen bonding as the sole determining factor in the elevated polymerization rates of the monomers in their study. The role of hydrogen abstraction, resulting in the formation of a cross-linked polymer, was supported by gel fraction measurements. Electronic effects were explored by investigating monomers substituted with benzyl substituent at the end-group and such groups were found to significantly enhance polymerization reactivity. Bowman et al. carried out several systematic variations on the structure of *N*-phenyl carbamate ethyl acrylates (PCEAs). In exploring the roles of the aliphatic spacer [10], Bowman et al. substituted the ethyl spacer of PCEA with all combinations of one and two methyl groups at the α and β positions. They found that mono-substitution at either or both positions led to little reduction in polymerization rate. However, dual substitution at the β position led to a twofold reduction in polymerization rate and dual substitution at the α position led to a fivefold reduction in polymerization rate. Both of these latter results suggest that a hydrogen abstraction mechanism, which predominantly occurs at the α position, contributes to the polymerization reactivity of these monomers.

Bowman et al. also investigated the roles of polarity, electronic, and resonance effects by systematically varying the substituents on the aromatic ring of PCEA [11]. To study the role of polarity they computed a Boltzmann-averaged molecular dipole in a similar manner to Jansen. Additionally, the contribution of molecular pre-organization to enhanced polymerization reactivity, via hydrogen bonding, was studied by FTIR monitoring of the N–H stretching frequency as a function of temperature. They found none of these effects were primary factors accounting for the enhanced polymerization reactivity for monomers of the PCEA type. The role of the molecular dipole was further investigated by Bowman in light of a possible solvent effect [12]. They again found no relationship between the computed molecular dipole and polymerization reactivity and only a minimal effect of solvent polarity. Since the bulk medium appeared to play a role in polymerization reactivity, at least in part, Bowman further investigated the role of solvent polarity with respect to the potential for π–π stacking of the aromatic rings and hydrogen bonding of the carbamate N–H bond for PCEA type monomers [13]. Reactivity differences were found for monomers whether in bulk or at dilution to 5 wt%, thus suggesting that there is a significant intramolecular conformational contribution to the elevated reactivity of PCEA type monomers. The authors noted that hydrogen bonding and π–π stacking contribute to enhanced reactivity. They also provided quantitative structure-functionality estimations of these effects to the enhanced reactivity of the monomer types in the study.

The estimation of functional group contributions to polymer properties is a well-known practice [14]. The estimation of the contributions of functional groups to monomer *reactivity* is not as common. Monomer reactivity is usually modeled by means of computational reaction modeling, of which there are numerous examples [15–18]. For instance, Aviyente et al. have modeled various reactions pertaining to the radical polymerization process for a series of acrylates possessing a variety of side groups including heteroatoms [15]. The reactions included initiation, propagation, chain transfer, and termination by disproportionation and coupling. These reactions were modeled using a combined DFT approach that made use of a 6-31G*+ basis and the B3LYP functional for initial geometry optimizations followed by a newer BMK (Bose Martin for kinetics) functional for single point optimizations involved in the calculation of barrier heights. The investigation resulted in qualitative agreement with experiment in the trend in reactivity for the monomers studied. Additionally, it was found that when polar side groups are attached to monomers, reaction pathways corresponding to chain transfer to inactivated monomer was competitive with propagation and that coupling was the most likely route for polymerization termination.

Another approach to monomer polymerization reactivity modeling has included the derivation of multivariate correlation equations that are descriptive of a property of interest, the so called quantitative structure–activity relationship (QSAR) approach. Typically the QSAR approach involves performing a multiple linear regression of a set of computed descriptor quantities onto an experimental property. Although the QSAR approach has been widely employed in drug discovery and other applications, it has seen relatively little use in modeling polymer reactivity.

For example, Toropov et al. used a graph theoretical approach to model the resonance (Q) and polar effects (e) on monomer activity in copolymerization reactions involving vinyl and (meth)acrylate type monomers [19]. Good qualitative agreement was found between the computed resonance and polarity parameters and those quantities derived from experiment, where test sets gave correlation coefficients as high as $r = 0.8283$.

In a related study Yu et al. expanded upon the graph theoretical approach to include monomer reactivity descriptors that were derived on the basis of quantum mechanical computation [20]. The descriptors were calculated using a B3LYP/6-31G(d,p) basis and included Mulliken atomic charges (and charge differences) of selected atoms, the molecular polarizability (α), the energies of the frontier molecular orbitals, and the total electronic energy. The correlation equations were derived using a multiple linear regression analysis (MLRA) for initial selection of descriptors, followed by an artificial neural network (ANN) treatment to derive the final predictive model. The authors found a good fit to the data in the MLRA analysis with training set multiple correlation coefficients of $R = 0.910$ for $\ln Q$ and $R = 0.960$ for e. The ANN treatment also resulted in an acceptable model for the reactivity parameters.

1.1. Objective and general approach

The reactivity studies of (meth)acrylate monomers by the Bowman and Jansen groups, coupled with the more recent successes in applying QSAR treatments to monomer reactivity, has strongly suggested to us that a QSAR approach could be used to explain monomer reactivity. Toward explaining the unusually fast reactivity of (meth)acrylate monomers bearing novel functionalities we have conducted a more thorough *a priori* search of descriptor space in the hope that we could derive a model of reactivity that was both predictive and explanatory. We anticipated that such a model would suggest structure features of monomers leading to a mechanism (or mechanisms) of ultra-fast polymerization. We have expanded on the approaches of Toropov and Yu to include topological descriptors derived from graph theory and explicitly quantum mechanical descriptors. In addition we have included several other descriptors from classes described as geometric, electrostatic, and thermodynamic; all derived from quantum mechanical calcula-

Table 1
Multiple correlation equation parameters and associated significance values for the single best three-descriptor correlation equation from the CODESSA analysis of maximum polymerization rates for 15 monomers polymerized under bulk conditions and those diluted in 1,4-dioxane to 5 wt%.

Exp. conditions and significance values	Index	Descriptor	Coefficient	Student's[a] *t*	VIF
Bulk					
$R^2 = 0.9365$[b]	Desc-1	Average bond order of an oxygen atom	17.52	8.873	2.15
$F = 54.11$[c]	Desc-2	Average bond order of an hydrogen atom	90.84	6.716	1.11
$R^2_{CV} = 0.8699$[d]	Desc-3	Surface area of the most negatively charged atom relative to the sum of negative charges (RNCS-ESP)	−0.2520	−5.617	2.24
$R^2_{adj.} = 0.9196$[e]		Intercept	−100.5	−7.993	
Dilute (5 wt%)					
$R^2 = 0.9839$[f]	Desc-4	Min. (>0.1) bond order of an oxygen atom	18.00	20.97	2.25
$F = 224.0$[c]	Desc-5	Min. partial charge for a carbon atom	−8.931	−4.009	1.84
$R^2_{CV} = 0.9746$[d]	Desc-6	Weighted partial positively charged surface area	5.909×10^{-3}	14.74	3.41
$R^2_{adj.} = 0.9796$[e]		Intercept	0.3396	2.407	

[a] All descriptors are significant at the $p < 0.005$ level with 14 degrees of freedom.
[b] The BMLR algorithm was used to derive the correlation.
[c] Fisher statistic. Both are significant at the $p < 0.001$ level with 14 and 11 degrees of freedom.
[d] Leave-one-out cross validated coefficient of multiple determination.
[e] Adjusted coefficient of multiple determination.
[f] The Heuristic algorithm was used to derive the correlation.

tions. We have also performed principle components and cluster analysis on our models to aid in our interpretation of the results.

2. Computational methodology

2.1. Molecular modeling

All monomer structures were modeled using the AM1 semiempirical quantum mechanical method as implemented in the program, AMPAC *with Graphical User Interface* [21]. Generation and analysis of descriptors and multiple correlation equations was performed using the program, CODESSA (Comprehensive Descriptors for Structural and Statistical Analysis) [22]. The values of several of the descriptors generated by CODESSA depend directly on the conformation of the structures for which they are computed. In order to most accurately depict the monomer conformation we assumed that the global energy minimum conformation was the most representative conformation. In order to approximate the global energy minimum conformation we performed a conformational analysis whereby each rotatable bond was rotated about either 180° or 360° (in 10° increments), depending on the geometry about the bond being rotated. The lowest energy conformations from these analyses were then subjected to a geometry optimization without constraints and characterized, having been found to exhibit zero negative eigenvalues. The geometry possessing the lowest computed enthalpy of formation (ΔH_f^{298}) and zero negative eigenvalues amongst all of those analyzed was considered to be the global energy minimum conformation for the monomer. These geometries were then analyzed within CODESSA.

2.2. Selection of data sets

The data for the QSAR derivation and analysis came from published literature articles from the same group of researchers operating under the same polymerization conditions with the hope of minimizing systematic error [9,10,13]. The polymerization conditions were photopolymerization using 0.5 wt% 2,2-dimethoxy-2-phenylacetophenone (DMPA) as the photoinitiator, and irradiation for 5–10 min at a wavelength of 365 nm. The temperatures at which the polymerizations were conducted were either 25 °C or 67 °C depending on the melting point of the monomer. We do not believe that the temperature difference would have generated significant unexplained variance in our models because it has been shown that the polymerization rates for these types of monomers are somewhat insensitive to temperature [9]. All structurally ambiguous monomers (i.e. mixtures of enantiomers) were eliminated from consideration as well.

2.3. Derivation of multiple correlation equations

As described previously [23], we used two algorithms within CODESSA for the computation of descriptors and generation of multiple correlation equations. Briefly, the algorithms build correlation equations through forward simple least squares regression, and are called Best Multilinear Regression (BMLR) and Heuristic. The algorithms perform preliminary elimination of descriptors with values that do not vary, are not defined for each monomer in the training set, or are not significantly correlated with the

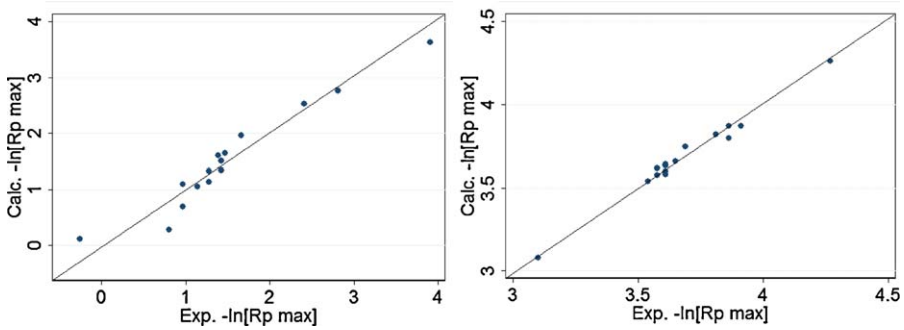

Fig. 1. Plots of the results of regression on maximum polymerization rates ($-\ln[R_{p\,max}]$) under bulk (a) and dilute (b) reaction conditions.

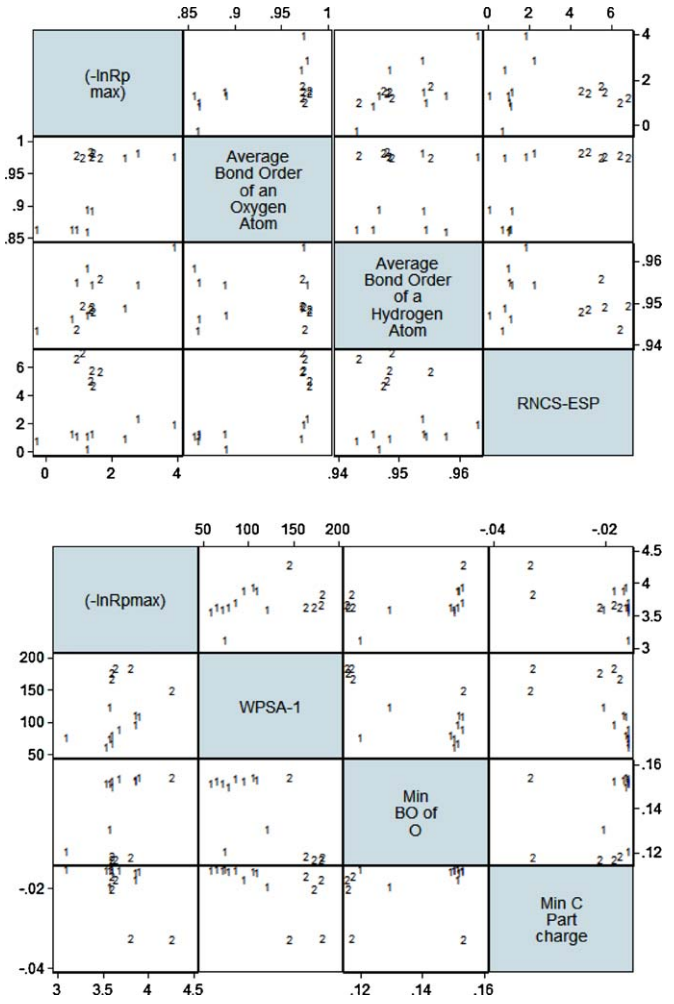

Fig. 2. Matrix plots of the cluster analysis of descriptor values plotted against experimental maximum polymerization rates ($-\ln[R_{p\max}]$) under bulk (upper) and dilute (lower) polymerization conditions.

defined property. Of the two algorithms the Hueristic algorithm has generally more stringent selection criteria for considering descriptors. For instance, in the BMLR analysis of monomers polymerized under bulk conditions the initial starting set consisted of 421 descriptors and the Heuristic algorithm started with 209 descriptors. Then the algorithms perform regression with the remaining descriptors, individually, on the property of interest provided that they do exhibit significant pair wise correlation with any other descriptor ($R^2_{i,j} < 0.1$). BMLR then iteratively builds correlation equations until successive iteration fails to improve the coefficient of multiple determination above a threshold value ($R^2_{\min} < 0.02$), retaining the best 400 equations in each iteration. Hueristic builds correlation equations by a similar process, except that the Hueristic algorithm optimizes the Fisher statistic (F-value) for the correlations equations and stops when it has reached a user specified maximum number of descriptors in the model. In the current study all correlation equations were limited to three descriptors due to the small size of the training sets. The 10 equations having the highest coefficients of multiple determination (BMLR) or F-value (Hueristic) in each iteration are reported as output. For our purposes the algorithm producing the best fit to the experimental data was retained, provided that the correlation equation contained no descriptors for which the threshold variance inflation factor (VIF = 5.0) was not exceeded.

Table 2
Cluster analysis groupings for the monomers of the training sets for the correlation equations obtained for bulk and dilute polymerization conditions.

Monomer	Bulk group	Dilute group
Benzyl acrylate	1	1
Benzyl carbamate ethyl acrylate	1	2
Cyclic carbonate acrylate	1	1
Ethyl linear carbonate acrylate	1	1
Hexyl acrylate	1	2
Methoxyethyl acrylate	1	1
n-Butyl carbamate ethyl acrylate	1	2
Phenyl carbamate ethyl acrylate	1	2
tert-Butyl carbamate (OCN) acrylate	1	2
Cyanoethyl acrylate	2	1
Hydroxyl butyl acrylate	2	1
Phenoxyethyl acrylate	2	1
Phenyl acrylate	2	1
Carboxyethyl acrylate	2	1
Hydroxyethyl acrylate	2	1

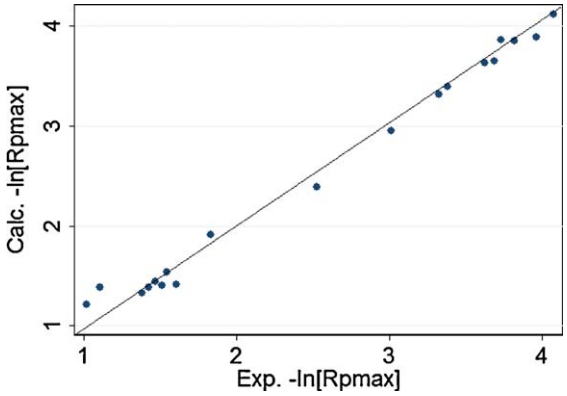

Fig. 3. Plot of the results of regression on maximum polymerization rates ($-\ln[R_{p\max}]$) under bulk conditions for monomers bearing carbamate functional groups.

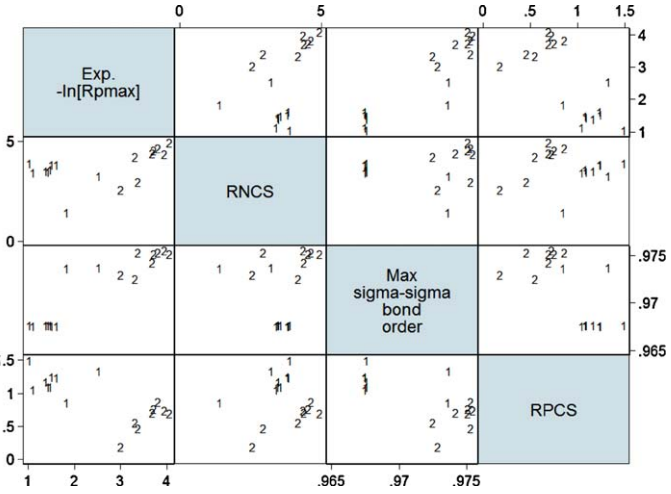

Fig. 4. Matrix plot of the cluster analysis of descriptor values plotted against experimental maximum polymerization rates ($-\ln[R_{p\max}]$) under bulk polymerization conditions for monomers containing a carbamate functional group.

3. Results

To discern between the contributions of intermolecular and intramolecular effects on the rates of polymerization of monomers Bowman polymerized fast-reacting monomers both in bulk and at 5 wt% dilution in 1,4-dioxane [13]. In an attempt to identify structural features that are either intramolecular or intermolec-

Table 3
Multiple correlation equation parameters and associated significance values for the single best three-descriptor correlation equation from the CODESSA analysis of bulk maximum polymerization rates for 17 monomers bearing a carbamate functional group.

Exp. conditions and significance values	Index	Descriptor	Coefficient	Student's[a] *t*	VIF
Bulk					
$R^2 = 0.9891$[b]	Desc-7	Surface area of the most negatively charged atom relative to the sum of negative charges (RNCS)	0.4861	12.28	1.08
$F = 393.7$[c]	Desc-8	Max. σ-σ bond order	217.8	16.68	2.07
$R^2_{CV} = 0.9800$[d]	Desc-9	Surface area of the most positively charged[f] atom relative to the sum of positive charges (RPCG)	−0.9293	−5.617	2.00
$R^2_{adj.} = 0.9865$[e]		Intercept	−210.0	−7.01	

[a] All descriptors are significant at the $p < 0.005$ level with 16 degrees of freedom.
[b] The BMLR algorithm was used to derive the correlation.
[c] Fisher statistic, significant at the $p < 0.001$ level with 16 and 13 degrees of freedom.
[d] Leave-one-out cross validated coefficient of multiple determination.
[e] Adjusted coefficient of multiple determination.
[f] Computed by the method of Zefirov, which is a geometric mean of Sanderson electronegativities.

Table 4
Groupings from the cluster analysis of the correlation for monomers containing carbamate functionality and polymerized under bulk conditions.

Monomer	Group
Phenyl-(NCO)-carbamate (α,α-dimethyl)-ethyl acrylate	1
Phenyl-(NCO)-carbamate (β,β-dimethyl)-ethyl acrylate	1
meta-Fluorophenyl-(NCO)-carbamate ethyl acrylate	1
meta-Methoxyphenyl-(NCO)-carbamate ethyl acrylate	1
ortho-Fluorophenyl-(NCO)-carbamate ethyl acrylate	1
ortho-Methoxyphenyl-(NCO)-carbamate ethyl acrylate	1
para-Fluorophenyl-(NCO)-carbamate ethyl acrylate	1
Phenyl-(NCO)-carbamate ethyl acrylate	1
para-Methoxyphenyl-(NCO)-carbamate ethyl acrylate	1
Benzyl-(NCO)-carbamate ethyl methacrylate	2
Benzyl-(OCN)-carbamate ethyl methacrylate	2
n-Butyl-(NCO)-carbamate ethyl methacrylate	2
Ethyl-(NCO)-carbamate ethyl methacrylate	2
Ethyl-(OCN)-carbamate ethyl methacrylate	2
Isopropyl-(NCO)-carbamate ethyl methacrylate	2
n-Propyl-(NCO)-carbamate ethyl methacrylate	2
t-Butyl-(NCO)-carbamate ethyl methacrylate	2

ular contributors to the polymerization rates we performed QSAR analyses on two sets of monomers that were polymerized under the bulk and dilute conditions described above. For these multiple correlation analyses the equation descriptors, coefficients, and associated significance values are listed in Table 1. The corresponding regression models are plotted in Fig. 1. As shown in Table 1 both the bulk and dilute polymerization correlation analyses resulted in a very good fit to the experimental data. Although the training set of monomers is relatively small, the adjusted coefficients of multiple determination ($R^2_{adj.}$) are acceptably close to the value of R^2 for the multiple correlation (within 80%). Also the values of R^2_{CV} are acceptably high, indicating relative insensitivity to removal of any of the members of the training set. The *F*-value for both the bulk and dilute models is statistically significant at the given level. Student's *t* test values indicate that the regression coefficients are better than zero at the given level of significance for all descriptors in both models. The variance inflation factors (VIFs) indicate that there is not significant intercorrelation amongst the descriptors since the maximum of these values is 3.41, with a mean value of 2.17, sufficiently below a critical value of 5.0. The relative negatively charged surface area descriptor (Desc-3) [24] is computed according to the following formula:

$$RNCS = SA_{MNeg}\frac{q_{MNeg}}{\sum qNeg}$$

where SA_{MNeg} is the surface area of the most negatively charged atom, q_{MNeg} is the charge of the most negatively charged atom, and $\sum q_{Neg}$ is the sum total of the negative charges of the atoms in the molecule. The bond order descriptors in the bulk model are computed from a population analysis of the density matrix within the semiempirical quantum mechanical formalism.

It is worthy to note that, in the bulk polymerization model all of the descriptors are whole-molecule descriptors, whereas in the dilute polymerization model two out of three descriptors are atom

Table 5
Multiple correlation equation parameters and associated significance values for the single best three-descriptor correlation equations from the CODESSA analysis of bulk maximum polymerization rates for nine *N*-phenyl carbamate acrylates and eight carbamate methacrylates.

Monomer training set significance values	Index	Descriptor	Coefficient	Student's[a] *t*	VIF
N-Phenyl carbamate acrylates					
$R^2 = 0.9947$[b]	Desc-10	Max. electrophilic reactivity index for an oxygen atom	-2.938×10^3	−26.78	2.53
$F = 312.6$[c]	Desc-11	Hydrogen bond donors charged (ESP) surface area (HDCA)	8.401×10^{-2}	14.87	1.33
$R^2_{CV} = 0.9773$[d]	Desc-12	Fractional positively charged (ESP) surface area (FPSA-3)	−40.00	−12.64	2.80
$R^2_{adj.} = 0.9799$[e]		Intercept	39.62	25.09	
Carbamate methacrylates					
$R^2 = 0.9994$[f]	Desc-13	Wiener index	-1.131×10^{-3}	−53.92	1.07
$F = 2176$[c]	Desc-14	Hydrogen bond acceptor surface area	0.1104	48.74	1.29
$R^2_{CV} = 0.9746$[d]	Desc-15	Max. internuclear repulsion for a C–C bond	−0.3022	−22.41	1.25
$R^2_{adj.} = 0.9989$[e]		Intercept	38.47	23.57	

[a] All descriptors are significant at the $p < 0.005$ level with 8 and 7 degrees of freedom.
[b] The BMLR algorithm was used to derive the correlation.
[c] Fisher statistic. Both are significant at the $p < 0.001$ level with 7 and 4 degrees of freedom.
[d] Leave-one-out cross validated coefficient of multiple determination.
[e] Adjusted coefficient of multiple determination.
[f] The BMLR algorithm was used to derive the correlation.

Table 6
Results of principal component analysis (PCA) of the QSAR models corresponding to bulk and dilute polymerization conditions, as well as PCA for the carbamate QSAR model and its subsets.

Exp. conditions and principal component	Descriptor	Eigenvector	Eigenvalue	Variance explained (%)	Cumulative variance explained (%)
Bulk					
PC1	Desc-1	0.6838	1.7329	0.5776	0.5776
	Desc-2	−0.1688			
	Desc-3	0.7099			
PC2	Desc-1	0.2677	1.0129	0.3376	0.9153
	Desc-2	0.9631			
	Desc-3	−0.0289			
PC3	Desc-1	−0.6788	0.2542	0.0847	1.0000
	Desc-2	0.2098			
	Desc-3	0.7037			
Dilute					
PC1	Desc-4	0.5506	2.0395	0.6798	0.6798
	Desc-5	0.5045			
	Desc-6	−0.6650			
PC2	Desc-4	−0.6521	0.7861	0.2620	0.9419
	Desc-5	0.7573			
	Desc-6	0.0346			
PC3	Desc-4	0.5211	0.1743	0.0581	1.0000
	Desc-5	0.4146			
	Desc-6	0.7460			
Carbamates					
PC1	Desc-7	0.1194	1.6770	0.5590	0.5590
	Desc-8	0.7113			
	Desc-9	−0.6927			
PC2	Desc-7	0.9707	1.0219	0.3406	0.8996
	Desc-8	0.0627			
	Desc-9	0.2318			
PC3	Desc-7	−0.2083	0.3011	0.1004	1.0000
	Desc-8	0.7001			
	Desc-9	0.6830			
N-Phenyl carbamates					
PC1	Desc-10	−0.6548	1.7734	0.5911	0.5911
	Desc-11	0.2491			
	Desc-12	0.7136			
PC2	Desc-10	0.3916	1.0316	0.3439	0.9350
	Desc-11	0.9194			
	Desc-12	0.0384			
PC3	Desc-10	0.6465	0.1951	0.0650	1.0000
	Desc-11	−0.3046			
	Desc-12	0.6995			
Carbamate methacrylates					
PC1	Desc-13	−0.4474	1.5916	0.5305	0.5305
	Desc-14	0.6450			
	Desc-15	0.6194			
PC2	Desc-13	0.8865	0.8573	0.2858	0.8163
	Desc-14	0.2282			
	Desc-15	0.4026			
PC3	Desc-13	0.1183	0.5511	0.1837	1.0000
	Desc-14	0.7293			
	Desc-15	−0.6793			

or bond specific descriptors. Thus, suggesting that the QSAR models are somewhat capable of recognizing the different reactivities under differing polymerization conditions.

To determine if there are natural groupings of descriptors as they relate structural similarities to the experimental data we performed a k means cluster analysis [25] (see Fig. 2) on the descriptor values. For the cluster analysis we specified that two clusters were to be generated using an iterative process that was begun by randomly choosing the center point of the clusters with a user-specified seed number used for reproducibility. The measure of the similarity or dissimilarity was the absolute value distance. As indicated in Fig. 2 there are two distinct groupings of descriptor values when comparing descriptors on a two-dimensional plot basis for both the bulk and dilute polymerization data. The compounds belonging to each group are listed in Table 2. From Table 2 a structural pattern emerges for the bulk polymerization data that indicates the members of group 1 are dominated by either the carbamates or the carbonates. The groupings for the dilute polymerization data appear even more distinctly divided on the basis of carbamate functionality. We interpret this as the model generally recognizing the difference in reactivity between those acrylate monomers bearing novel functionality and more traditional acrylate monomers. A notable exception to this pattern is hexyl acrylate, which is grouped with the faster reacting carbamate acrylates.

In our attempt to derive a correlation that could be used to suggest some molecular structural explanation for the enhanced reactivity of acrylate monomers bearing novel functionality we narrowed our training set of monomers to only those containing carbamate functional groups. The data set consists of bulk polymerization studies of a series of 17 monomers, which were polymerized under the same reaction conditions to those described above. The results are listed in Table 3 and the corresponding fitted plot appears in Fig. 3. As indicated by Table 3 and Fig. 3 the BMLR algorithm found a strong and statistically relevant fit to the

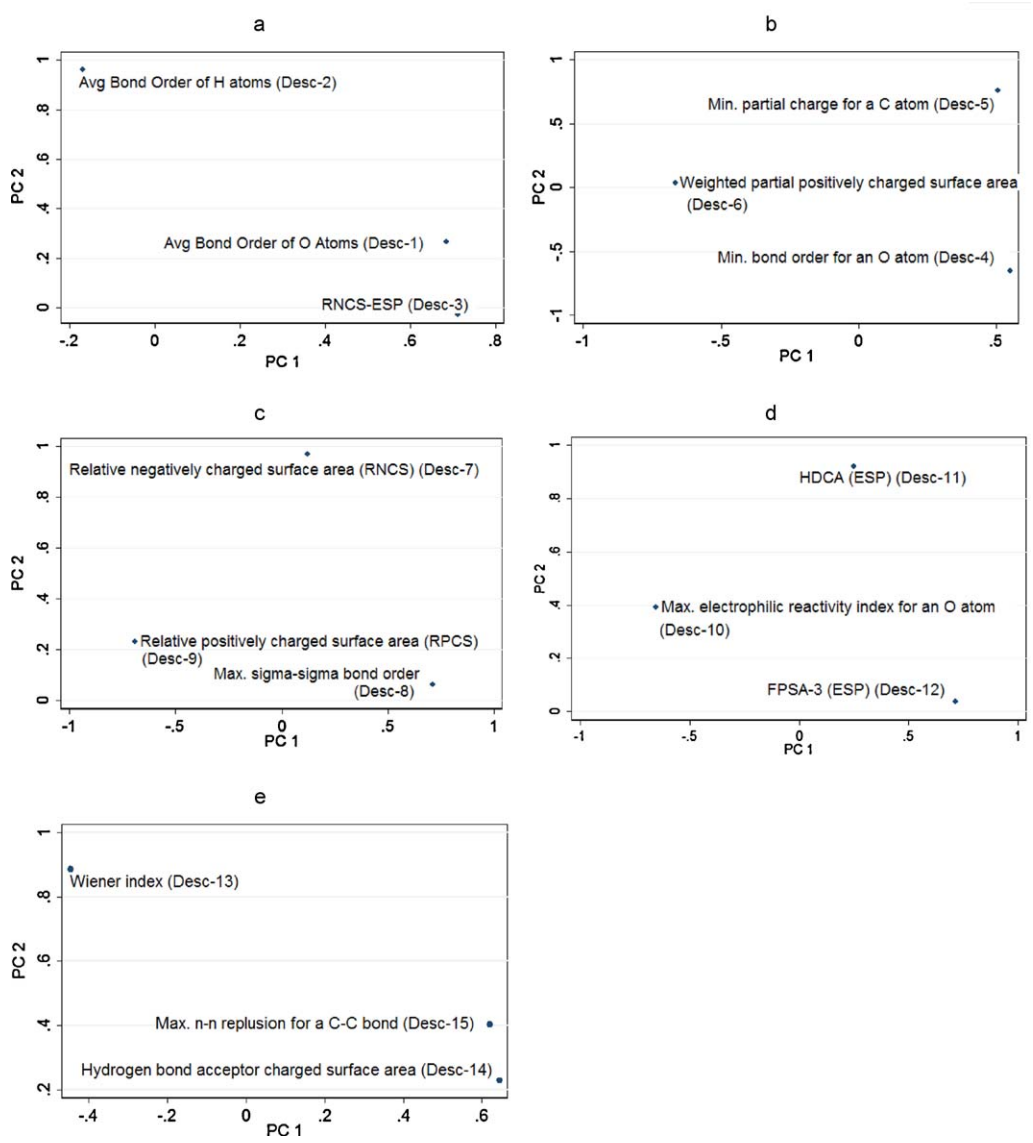

Fig. 5. Score plots from the principal component analysis of the descriptors in the correlation equations for monomers polymerized under bulk conditions (a), dilute conditions (b), bulk conditions with carbamate functionality (c), bulk conditions with *N*-phenyl carbamate and acrylate functionality (d), and bulk conditions with carbamate and methacrylate functionality (e). The marker labels indicate the ranked order of reactivity from fast to slow in increasing order.

experimental data. Cluster analysis was also completed on this training set. The results are plotted in Fig. 4 in a pair wise comparison that again indicates that there are distinct groupings of descriptor values as compared to the maximum polymerization rates and as the descriptors are compared with one another. Analysis of the monomers in each group, as listed in Table 4, suggests that this QSAR model recognizes differences in reactivity on the basis of a few distinct functional group differences amongst monomer types. The members of group one are uniformly *N*-phenyl carbamates with acrylate functionality. The members of group two are uniformly carbamate methacrylates that lack the *N*-phenyl functionality.

So that we could examine the portion of the variance represented by each descriptor independently and attempt to detect any underlying trends in our regression models we performed multiple regressions analysis (Table 5) and subsequent principal component (PC) analysis on our QSAR models. The training sets and corresponding QSAR models chosen for principle components analysis include the bulk and dilute polymerization models, the carbamate functional monomer set, as well as the two subgroups of carbamate monomers as indicated by the cluster analysis of the carbamate monomer QSAR model (the *N*-phenyl carbamate acrylates and the carbamate methacrylates). It should be noted that although the size of the subgroup training sets is small, it has been shown that QSAR analyses on similar sized training sets have yielded useful results [26]. The eigenvectors, eigenvalues, and portion of the variance explained by each of the principal components for all multiple regression models are listed in Table 6. In each study group the first two PCs accounted for over 80% of the total variance in the model, thus only the first two PCs were included for analysis in the score plots and the loadings plots for each study group (see Figs. 5 and 6, respectively). For the monomers polymerized under bulk conditions (Figs. 5a and 6a) the average bond order of an oxygen atom (Desc-1) and the relative negatively charged surface area (Desc-3) appear to have the same effect as these descriptors are closely associated with one another in Fig. 5a. Based on a comparison to Fig. 6a it appears that for slower polymerizing monomers the average bond order of oxygen is higher and that for faster monomers the average oxygen bond order is lower. A possible interpretation is that for the faster carbamate monomers the nitrogen of the

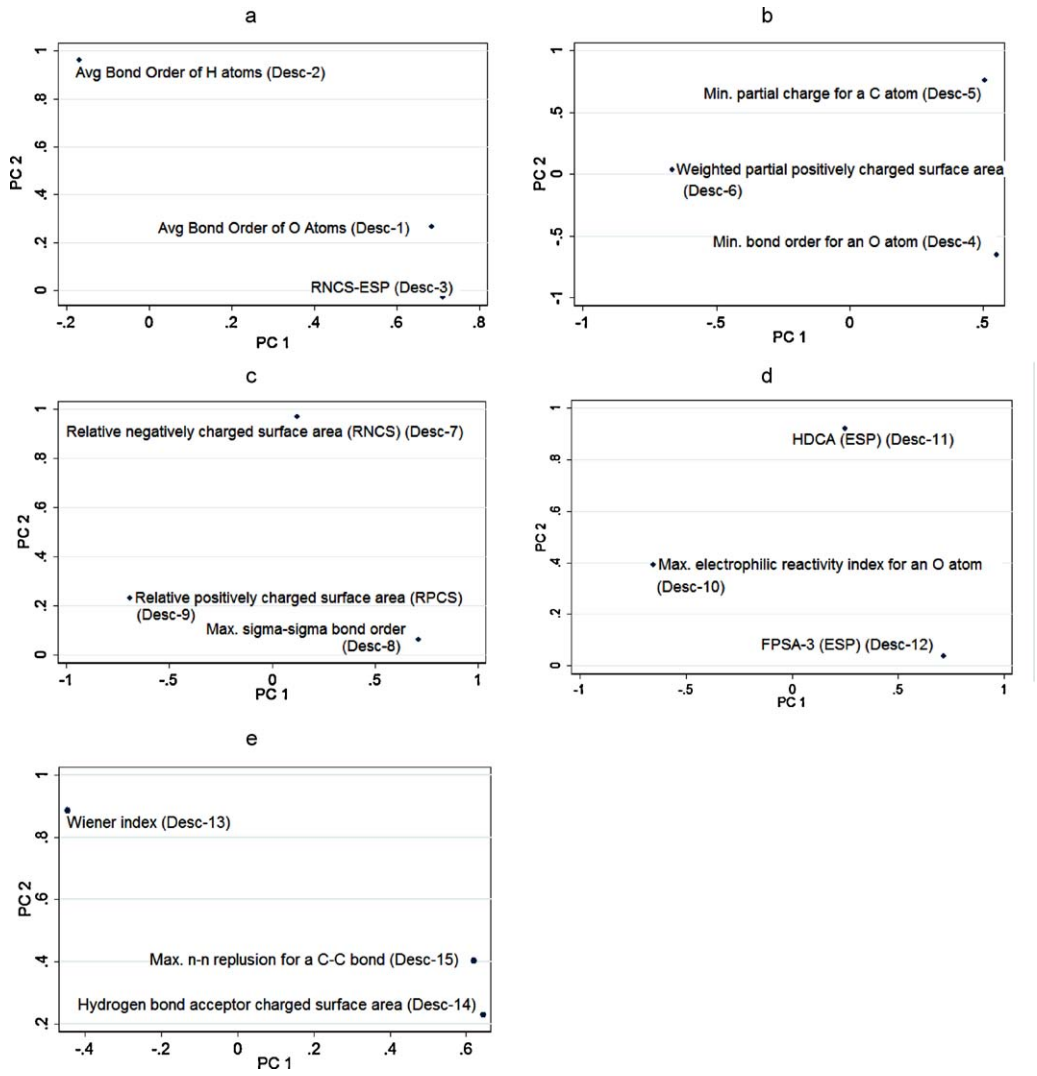

Fig. 6. Loading plots from the principal component analysis of the descriptors in the correlation equations for monomers polymerized under bulk conditions (a), dilute conditions (b), bulk conditions with carbamate functionality (c), bulk conditions with *N*-phenyl carbamate and acrylate functionality (d), and bulk conditions with carbamate and methacrylate functionality (e).

carbamate donates electron density to the carbonyl group of the carbamate, thus lowering the bond order of the carbamate carbonyl bond. That this is possible for the carbamate bearing monomers suggests that the descriptor functions to differentiate the faster carbamate acrylate monomers from the generally slower traditional acrylates. The importance of a contribution of electron density by the nitrogen to the carbamate carbonyl correlation speaks to the results of Kilambi for the acid inhibition of acrylates bearing novel functionalities, including carbamate and cyclic carbonate [27]. As the nitrogen of the carbamate donates electron density to the carbonyl group, the build-up of negative charge on the oxygen atom makes it a site for intermolecular hydrogen bonding, as well as a site for protonation under acidic conditions. If the amide group of the carbamate is participating in extensive hydrogen bonding under neutral conditions, such hydrogen bonding could lead to rate enhancing preorganization as proposed by Bowman and Jansen and others [7–9]. Protonation of the carbonyl oxygen of the carbamate would thus weaken hydrogen bonding and preorganization leading to a greater reduction in rate due to acid than that shown for traditional acrylates. Monomers lacking the carbamate functionality would lack the corresponding site for protonation, subsequently would not be undergoing the same hydrogen bonding, and should be less hindered by the presence of acid. For the same correlation the average bonds order of a hydrogen atom descriptor (Desc-2) carries much greater influence in the second principal component and appears to be a positive predictor of slower polymerization rates in PC2. It would thus appear that this descriptor indicates that as the average covalent bond to a hydrogen atom becomes stronger the polymerization rate for the monomer is slower. This parallels the suggestions by Bowman [10] and Jansen [8] that a hydrogen abstraction mechanism may be taking place. Greater hydrogen abstraction by way of more labile hydrogen atoms could lead to decreased rates for termination and possibly the formation of an effective solvent cage via radical cross linking of the polymer, thus leading to enhanced polymerization rate.

For the monomers polymerized under dilute conditions the score plots and corresponding loading plots are listed in Figs. 5b and 6b, respectively. The descriptors are the minimum bond order of an oxygen atom (Desc-4) and the minimum charge of a carbon atom (Desc-5) and the weighted partially positively charged surface area (Desc-6). For this correlation, principal component analysis has all three of the descriptors weighted approximately equally in the first principal component. In the second principal component Desc-5 and Desc-6 carry most of the influence and act in opposing ways. Comparison to the cluster analysis (Fig. 2 and Table 2) for this correlation suggests that these descriptors func-

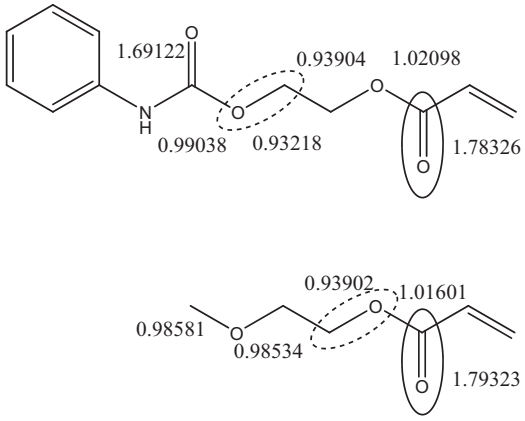

Fig. 7. Structures of representative monomers, phenyl carbamate ethyl acrylate (top) and methoxyethyl acrylate (bottom), from the training set of monomers polymerized under dilute conditions. The structures have the bond orders for bonds to oxygen atoms indicated. The minimum and maximum bond orders for a bond to an oxygen atom are circled with dashed and solid lines, respectively.

tion to differentiate the faster carbamates from the more traditional acrylates on the basis of differences in the ways in which these monomers undergo intermolecular interactions. In the context of CODESSA charges may be read directly from quantum mechanical calculations or they may be computed by the method of Zefirov. The latter method involves computing the charge of an atom as the geometric mean of Sanderson electronegativities of all of the atoms bonded to the atom for which the charge is being calculated. Thus, for any given atom in a functional group the Zefirov partial charge will always be the same regardless of whether that functional group is in a slightly different electronic environment in two given molecules. Taken together with the cluster analysis for this descriptor it appears that the operation of the descriptor within the correlation is to differentiate the generally faster carbamates from the slower traditional acrylates on the basis of functional group differences. Using CODESSA the oxygen bond order descriptor (Desc-4) was mapped onto the structure of several monomers in the correlation training set. Representative examples of carbamate and traditional acrylate monomers from this training set where Desc-4 was mapped onto the monomer structure are shown in Fig. 7. As indicated in Fig. 7 the minimum bond order for a bond to an oxygen atom (Desc-4) corresponds to the non-carbonyl oxygen atom of the carbamate functional group for the carbamate acrylate monomer. For the traditional acrylate Desc-4 corresponds to the non-carbonyl bond of the acrylate functional group. Taken together with the cluster analysis for this correlation it appears that this descriptor also operates within the correlation to differentiate monomers on the basis of functional group differences. The results of PCA on the QSAR for acrylate monomers containing only carbamate functionality are given in Table 6 and Figs. 5c and 6c. In PC1 the descriptors relative negatively charged surface area (Desc-7) and the relative positively charged surface area (Desc-9) bear loadings of opposite signs. The complementary nature of these descriptors suggests that they function within the correlation to describe how the monomers interact with each other under bulk polymerization conditions. The results of PCA on the QSAR for the *N*-phenyl carbamate acrylate monomers are given in Table 6 and Figs. 5d and 6d. The score plot (Fig. 5d) for this PCA shows almost no differentiation between fast and slow *N*-phenyl carbamate acrylate monomers. The loadings plot (Fig. 6d) suggests that the descriptors function within the correlation to differentiate reactivity potential (Desc-10) from intermolecular interactions (Desc-11 and Desc-12). It appears by comparison of Figs. 5d and 6d that the more surface area that a monomer possesses which bears partial positive charge, and the more surface area from hydrogen bond donors, the slower reacting the monomer. Whereas, faster reacting monomers are positively correlated with Desc-10 (maximum electrophilic reactivity index for an oxygen atom). This descriptor was developed by Fukui for describing the tendency of a molecule to act as an electrophile in a chemical reaction [28]. The descriptor is calculated according to the following formula:

$$E_A = \sum_{j \in A}^{n} \frac{C_{jLUMO}^2}{\varepsilon_{LUMO} + 10}$$

where the summation is performed over the coefficients to the lowest unoccupied molecular orbital (LUMO) centered on the atom of interest, and ε_{LUMO} is the energy of the LUMO. The pertaining oxygen atom for every monomer in the QSAR training set for this correlation was the oxygen atom of the acrylate functional group. A plot for the LUMO for one monomer of this training set is represented in Fig. 8. As indicated in Fig. 8 the LUMO is located on the acrylate functional group. The location of this MO suggests that these monomers are undergoing a reaction as an electrophile at the acrylate carbon–carbon double bond. Such a Michael addition has been investigated by Bowman who found that acrylate monomers bearing carbamate functionality exhibited a high degree of Michael addition reactivity to thiols catalyzed by triethylamine [29]. For novel monomers undergoing polymerization under photoinitiated radical conditions a nucleophilic species has not been proposed, although Jansen et al. have modeled a propagating radical at the DFT level [8]. Using a B3LYP/6-31G* basis they computed a negative charge for their modeled propagating radical, thus suggesting that the propagating species may have some negatively charged character. The anionic nature of the propagating species was further investigated by Bowman who found a significant inhibition by strong acid when polymerized under photoinitiated radical conditions [27]. Thus, it appears that there is a Michael addition component to the polymerization that is occurring at the acrylate functional group and this idea is supported by our findings.

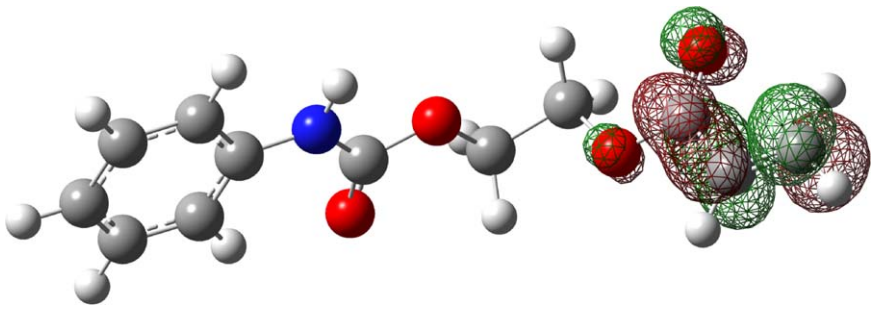

Fig. 8. Plot of the lowest unoccupied molecular orbital (LUMO) on the structure of the phenyl carbamate ethyl acrylate monomer. The location of the LUMO is representative of the *N*-phenyl carbamate acrylate monomers.

4. Conclusions

The QSAR analysis of the maximum polymerization rates of a series of structurally similar (meth)acrylate monomers bearing carbamate functionality has resulted in sound and chemically reasonable models. The descriptors that appear in these models are generally reflective of much experimental work that has been done to understand their unusually fast polymerization reactivity of these types of monomers. A notable exception to this statement lies in Desc-14 from the carbamate methacrylate model. The positive loading of this descriptor from its corresponding PCA analysis suggests that as the hydrogen bond donor surface area increases for these monomers, they polymerize more slowly. This appears to contradict the results of Jansen who showed evidence for the rate enhancing contribution of hydrogen bonding through molecular pre-organization [8]. Bowman et al. noted that while hydrogen bonding is a contributing factor, experiments based on the FTIR stretching frequencies for N–H bonds gave no definitive conclusions for the contribution of hydrogen bonding for *N*-alkyl carbamate methacrylates [9]. A likely reason for the discrepancy in this QSAR lies in the small size of the training set used to derive the corresponding multiple correlation equation. In the absence of more experimental data for alkyl carbamate methacrylate monomers little more can be done and conclusions regarding QSAR analysis of monomers of this type are tentative.

Although a definitive mechanistic explanation for the unusually fast reactivity exhibited by (meth)acrylate monomers bearing novel functional groups was not presented these results suggest a number of possibilities. We have computationally explored a number of these possibilities and are preparing a manuscript on our findings.

Acknowledgement

This work was supported by NIH grant 10959 from NIDCR.

Appendix A. Supplementary data

Supplementary data associated with this article can be found, in the online version, at doi:10.1016/j.jmgm.2010.12.009.

References

[1] A. Andrzejewska, M. Andrzejewski, Polymerization kinetics of photocurable acrylic resins, J. Polym. Sci. Part A: Polym. Chem. 36 (1998) 665–673.
[2] C. Decker, K. Moussa, Real-time kinetic study of laser-induced polymerization, Macromolecules 22 (12) (1989) 4455–4462.
[3] C. Decker, K. Moussa, Eur. Polym. J. 26 (4) (1990) 393–401.
[4] C. Decker, K. Moussa, A new class of highly reactive acrylic monomers. 1. Light-induced polymerization, Makromol. Chem. Rapid Commun. 11 (1990) 159–167.
[5] C. Decker, K. Moussa, A new class of highly reactive acrylic monomers. 2. Light-induced copolymerization with difunctional oligomers, Makromol. Chem. 192 (1991) 507–522.
[6] C. Decker, K. Moussa, Eur. Polym. J. 27 (9) (1991) 881–889.
[7] C.A. Guymon, C.N. Bowman, Kinetic analysis of polymerization rate acceleration during the formation of polymer/smectic liquid crystal composites, Macromolecules 30 (18) (1997) 5271–5278.
[8] J.F.G.A. Jansen, A.A. Dias, M. Dorschu, B. Coussens, Fast monomers: factors affecting the inherent reactivity of acrylate monomers in photoinitiated acrylate polymerization, Macromolecules 36 (11) (2003) 3861–3873.
[9] K.A. Berchtold, J. Nie, J.W. Stansbury, B. Hacioglu, E.R. Beckel, C.N. Bowman, Novel monovinyl methacrylic monomers containing secondary functionality for ultrarapid polymerization: steady-state evaluation, Macromolecules 37 (9) (2004) 3165–3179.
[10] E.R. Beckel, J.W. Stansbury, C.N. Bowman, Effect of aliphatic spacer substitution on the reactivity of phenyl carbamate acrylate monomers, Macromolecules 38 (8) (2005) 3093–3098.
[11] E.R. Beckel, J. Nie, J.W. Stansbury, C.N. Bowman, Effect of aryl substituents on the reactivity of phenyl carbamate acrylate monomers, Macromolecules 37 (11) (2004) 4062–4069.
[12] H. Kilambi, E.R. Beckel, K.A. Berchtold, J.W. Stansbury, C.N. Bowman, Influence of molecular dipole on monoacrylate monomer reactivity, Polymer 46 (2005) 4735–4742.
[13] H. Kilambi, J.W. Stansbury, C.N. Bowman, Deconvoluting the impact of intermolecular and intramolecular interactions on the polymerization kinetics of ultrarapid mono(meth)acrylates, Macromolecules 40 (1) (2007) 47–54.
[14] D.W. Van Krevelen, Properties of Polymers, Their Estimation and Correlation with Chemical Structure, Elsevier, Amsterdam, 1976.
[15] I. Degirmenci, D. Avci, V. Aviyente, Density functional theory study of free-radical polymerization of acrylates and methacrylates: structure–reactivity relationship, Macromolecules 40 (26) (2007) 9590–9602.
[16] S. Bebe, X. Yu, R.A. Hutchinson, L.J. Broadbelt, Estimation of free radical polymerization rate coefficients using computational chemistry, Macromol. Symp. 243 (2006) 179–189.
[17] P.M. Kazmaier, K.A. Moffat, M.K. Georges, R.P.N. Veregin, G.K. Hamer, Free-radical polymerization for narrow-polydispersity resins. Semiempirical molecular orbital calculations as a criterion for selecting stable free-radical reversible terminators, Macromolecules 28 (6) (1995) 1841–1846.
[18] D.M. Philipp, R.P. Muller, I. Goddard, W.A. Storer, J. McAdon, M. Mullins, Computational insights on the challenges for polymerizing polar monomers, J. Am. Chem. Soc. 124 (34) (2002) 10198–10210.
[19] A.A. Toropov, V.O. Kudyshkin, N.L. Voropaeva, I.N. Ruban, S.S. Rashidova, QSPR modeling of the reactivity parameters of monomers in radical copolymerizations, J. Struct. Chem. 45 (6) (2004) 945–950.
[20] X. Yu, B. Yi, X. Wang, Quantitative structure–property relationships for the reactivity parameters of acrylate monomers, Eur. Polym. J. 44 (2008) 3997–4001.
[21] AMPAC 8 with Graphical User Interface, Semichem Inc., Box 1649, Shawnee, KS 66222.
[22] CODESSA 2.7.8, Semichem Inc., Box 1649, Shawnee, KS 66222.
[23] J.A. Morrill, E.F.C. Byrd, Development of quantitative structure property relationships (QSPRs) for predictive modeling and design of energetic materials, J. Mol. Graph. Model. 27 (2008) 349–355.
[24] D.T. Stanton, P.C. Jurs, Development, Use of charged partial surface area structural descriptors in computer-assisted quantitative structure–property relationship studies, Anal. Chem. 62 (21) (1990) 2323–2329.
[25] StataCorp, Stata Statistical Software: Release 10, StataCorp LP, College Station, TX, 2007.
[26] P. Thipnate, J. Liu, S. Hannongbua, A.J. Hopfinger, 3D pharmacophore mapping using 4D QSAR analysis for the cytotoxicity of lamellarins against human hormone-dependent T47D breast cancer cells, J. Chem. Inf. Model. 49 (10) (2009) 2312–2322.
[27] H. Kilambi, D. Konopka, J.W. Stansbury, C.N. Bowman, Factors affecting the sensitivity to acid inhibition in novel acrylates characterized by secondary functionalities, J. Polym. Sci. Part A: Polym. Chem. 45 (2007) 1287–1295.
[28] K. Fukui, Theory of Orientation and Stereoselection, Springer-Verlag, Berlin, 1975.
[29] E.R.S.J.W. Beckel, C.N. Bowman, Evaluation of a potential ionic contribution to the polymerization of highly reactive (meth)acrylate monomers, Macromolecules 38 (23) (2005) 9474–9481.